Chromophore Formation in DsRed Occurs by a Branched Pathway

Rita L. Strack,[†,§] Daniel E. Strongin,[‡,§] Laurens Mets,[‡] Benjamin S. Glick,*[‡] and Robert J. Keenan*[†]

Department of Biochemistry and Molecular Biology and Department of Molecular Genetics and Cell Biology, The University of Chicago, Chicago, Illinois 60637

Received April 9, 2010; E-mail: bsglick@uchicago.edu; bkeenan@uchicago.edu

Abstract: Like GFP, the fluorescent protein DsRed has a chromophore that forms autocatalytically within the folded protein, but the mechanism of DsRed chromophore formation has been unclear. It was proposed that an initial oxidation generates a green chromophore, and that a final oxidation yields the red chromophore. However, this model does not adequately explain why a mature DsRed sample contains a mixture of green and red chromophores. We present evidence that the maturation pathway for DsRed branches upstream of chromophore formation. After an initial oxidation step, a final oxidation to form the acylimine of the red chromophore is in kinetic competition with a dehydration to form the green chromophore. This scheme explains why green and red chromophores are alternative end points of the maturation pathway.

Introduction

Fluorescent proteins undergo autocatalytic reactions that produce a variety of chromophores.[1−4] In GFP, the green chromophore is formed in several chemical steps (reviewed in refs 5, 6). First, the amide nitrogen of Gly67 attacks the carbonyl carbon of residue 65, forming an initial heterocycle. Subsequent oxidation and dehydration reactions generate an imidazolinone ring that is conjugated to the side chain of Tyr66. In the commonly used derivatives of wild-type (WT) GFP, deprotonation of the phenolic group yields an anionic green chromophore with absorbance and emission maxima of ∼480 and ∼510 nm, respectively.[7,8] DsRed has a similar reaction cycle but undergoes an additional oxidation to form an acylimine. This modification extends the conjugated π system and yields red-shifted absorbance and fluorescence maxima of ∼560 and ∼585 nm, respectively.[9,10] During maturation of tetrameric WT DsRed, green fluorescence appears early and then declines as red fluorescence appears.[11] These findings led to the conventional model in which an anionic green chromophore is a precursor to the red chromophore[1,2,11,12] (Scheme 1A).

Intriguingly, even after prolonged incubation, a DsRed sample contains a mixture of green and red chromophores. About half of the total chromophores in mature WT DsRed are green.[9,13] However, fluorescence emission from mature WT DsRed is mainly red due to intratetramer fluorescence resonance energy transfer (FRET).[11] Formation of the red chromophore lags behind formation of the green chromophore, so as red fluorescence appears, intratetramer FRET progressively suppresses the green fluorescence.[14] Verkhusha and colleagues made the key observation that the amount of green chromophore continues to increase throughout maturation, and never decreases as would be expected if the green chromophore were a precursor to the red chromophore.[14] These results are at odds with the conventional model.

To explain the existence of two distinct end points in the DsRed maturation pathway, Verkhusha and colleagues[14] proposed a modification of the conventional model. The concept is that deprotonation of the phenolic group is slow and irreversible, and is in competition with a second oxidation reaction that forms the red chromophore (Scheme 1B). Consistent with this model, the authors observed a transient blue species that absorbs maximally just above 400 nm, which is close to the absorbance peak of the neutral (protonated) GFP chromophore.[7,8] The blue species appeared early during matura-

† Department of Biochemistry and Molecular Biology, The University of Chicago.

§ These authors contributed equally.

‡ Department of Molecular Genetics and Cell Biology, The University of Chicago.

(1) Day, R. N.; Davidson, M. W. *Chem. Soc. Rev.* **2009**, *38*, 2887–2921.
(2) Remington, S. J. *Curr. Opin. Struct. Biol.* **2006**, *16*, 714–721.
(3) Sample, V.; Newman, R. H.; Zhang, J. *Chem. Soc. Rev.* **2009**, *38*, 2852–2864.
(4) Wiedenmann, J.; Oswald, F.; Nienhaus, G. U. *IUBMB Life* **2009**, *61*, 1029–1042.
(5) Craggs, T. D. *Chem. Soc. Rev.* **2009**, *38*, 2865–2875.
(6) Wachter, R. M. *Acc. Chem. Res.* **2007**, *40*, 120–127.
(7) Brejc, K.; Sixma, T. K.; Kitts, P. A.; Kain, S. R.; Tsien, R. Y.; Ormö, M.; Remington, S. J. *Proc. Natl. Acad. Sci. U.S.A.* **1997**, *94*, 2306–2311.
(8) Chattoraj, M.; King, B. A.; Bublitz, G. U.; Boxer, S. G. *Proc. Natl. Acad. Sci. U.S.A.* **1996**, *93*, 8362–8367.
(9) Gross, L. A.; Baird, G. S.; Hoffman, R. C.; Baldridge, K. K.; Tsien, R. Y. *Proc. Natl. Acad. Sci. U.S.A.* **2000**, *97*, 11990–11995.
(10) Wall, M. A.; Socolich, M.; Ranganathan, R. *Nat. Struct. Biol.* **2000**, *7*, 1133–1138.

(11) Baird, G. S.; Zacharias, D. A.; Tsien, R. Y. *Proc. Natl. Acad. Sci. U.S.A.* **2000**, *97*, 11984–11989.
(12) Terskikh, A.; Fradkov, A.; Ermakova, G.; Zaraisky, A.; Tan, P.; Kajava, A. V.; Zhao, X.; Lukyanov, S.; Matz, M.; Kim, S.; Weissman, I.; Siebert, P. *Science* **2000**, *290*, 1585–1588.
(13) Garcia-Parajo, M. F.; Koopman, M.; van Dijk, E. M. H. P.; Subramaniam, V.; van Hulst, N. F. *Proc. Natl. Acad. Sci. U.S.A.* **2001**, *98*, 14392–14397.
(14) Verkhusha, V. V.; Chudakov, D. M.; Gurskaya, N. G.; Lukyanov, S.; Lukyanov, K. A. *Chem. Biol.* **2004**, *11*, 845–854.

Scheme 1. Models for Chromophore Maturation in DsRed[a]
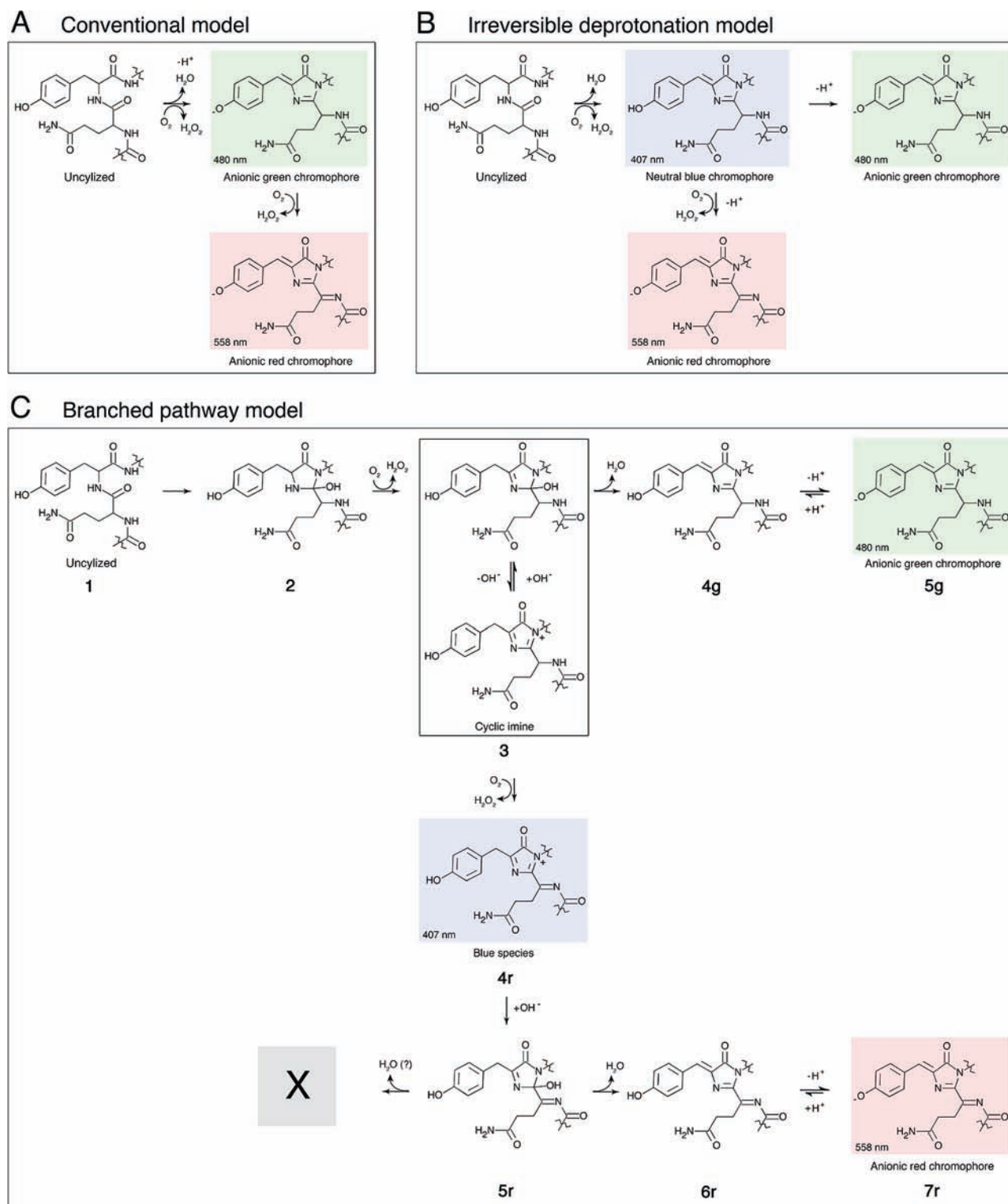
[a] Reactions involving the Gln66-Tyr67-Gly68 tripeptide are shown. (A) Conventional model. Cyclization, dehydration, initial oxidation, and deprotonation generate an anionic green chromophore, which is converted by a final oxidation to the red chromophore. Adapted from ref 2. (B) Irreversible deprotonation model. Cyclization, dehydration, and initial oxidation generate a neutral blue chromophore. Deprotonation of the neutral blue chromophore irreversibly forms the anionic green chromophore. Alternatively, a final oxidation of the neutral blue chromophore followed by deprotonation forms the red chromophore. Adapted from ref 14. (C) Our branched pathway model. The uncyclized tripeptide **1** is cyclized to **2**, which is the substrate for the initial oxidation. Oxidation may occur via an α-enolate intermediate[17,31] (not shown). The product of the initial oxidation is a hydroxylated cyclic imine, which is in rapid equilibrium with the cyclic imine. This equilibrium mixture **3** lies at the branch point in the pathway. Dehydration of the hydroxylated cyclic imine followed by deprotonation forms the anionic green chromophore **5g**. Alternatively, a final oxidation of the cyclic imine generates the blue species **4r**, and then dehydroxylation to **5r** is followed by dehydration to **6r**, which deprotonates to the red chromophore **7r**. An unknown side reaction of **5r** generates a nonabsorbing species ("X").

tion and then disappeared as the red chromophore appeared, suggesting that the blue species is on pathway to red.[14] This irreversible deprotonation model inspired the engineering of blue-to-red "fluorescent timer" variants of DsRed.[15] Yet the irreversible deprotonation model has limitations. Most notably, it makes the unlikely assumption that the anionic green chromophore never becomes protonated even on a time scale of months.

More recent studies from the same group indicate that in blue-to-red fluorescent timers, the blue species is not actually the anionic green chromophore, but rather a partial chromophore comprising the acylimine conjugated to the heterocycle.[16] This new concept can probably be extended to the blue species that was originally seen during DsRed maturation. However, the postulated maturation scheme for the fluorescent timers[16] fails to explain why many of the mature DsRed molecules have green chromophores. Thus, the older irreversible deprotonation model (Scheme 1B) has been the only attempt to explain the chromophore composition of mature DsRed.

To reconcile these various findings, we propose a novel branched pathway model that was inspired by recent studies of GFP maturation. Wachter and colleagues provided evidence that the GFP chromophore matures not by dehydration followed by oxidation, as had been thought, but rather by oxidation followed by dehydration.[17−19] This idea is recapitulated in our model for DsRed maturation (Scheme 1C). Cyclization of **1** to **2** is followed by an initial oxidation to generate intermediate **3**, which is suggested to be an equilibrium mixture of a cyclic imine with a hydroxylated cyclic imine.[17] Dehydration of the hydroxylated cyclic imine yields the neutral (protonated) GFP chromophore **4g**, and then rapid deprotonation yields the anionic green chromophore **5g**. We have extended this model to DsRed by postulating that dehydration of intermediate **3** is in competition with a final oxidation that generates the acylimine. To account for the existence of a blue species, we postulate that the substrate for the final oxidation is the cyclic imine (Scheme 1C), because oxidation of the cyclic imine would yield a conjugated species **4r** that could produce blue fluorescence. A somewhat different structure was proposed for the blue intermediate in blue-to-red fluorescent timers,[16] but the reported structural data are also consistent with **4r**. In our scheme, **4r** needs to be hydroxylated to **5r** to provide a substrate for dehydration to the neutral (protonated) chromophore **6r**, which is then rapidly deprotonated to the anionic red chromophore **7r**. We depict the **4r**-to-**5r** hydroxylation as being effectively unidirectional because our data confirm previous reports of a colorless kinetic intermediate between the blue species and the red chromophore.[14,15] Thus, the branched pathway model in Scheme 1C incorporates a host of observations from studies of GFP, wild-type DsRed, and DsRed variants, and it can explain why DsRed maturation yields green and red chromophores as stable end points.

Scheme 1C is a working hypothesis that can be tested at various levels of detail. We have focused here on the central

concept of this model, namely, that a branch point intermediate can undergo either a dehydration to produce the green chromophore, or a final oxidation to produce a blue species that is a precursor to the red chromophore. We have tested four specific predictions. The first prediction is that selectively slowing the dehydration of **3** to **4g** should favor the red branch of the pathway. The second prediction is that selectively slowing the oxidation of **3** to **4r** should favor the green branch of the pathway. The third prediction is that both of the oxidation steps in the maturation pathway should occur upstream of dehydration. The fourth prediction is that the blue species **4r** should be produced by the final oxidation step, and should be a precursor to the red chromophore but not to the green chromophore. All four predictions were confirmed. The combined results rule out previous models, and they match Scheme 1C qualitatively and quantitatively. These data solve a long-standing puzzle about the composition of mature DsRed.

Results

A Rapidly Maturing Soluble DsRed Variant as a Substrate for Analysis. We performed this analysis with a tetrameric DsRed variant called DsRed.T7, which was generated from the non-aggregating DsRed-Max[20] by an M66Q reversion that restored the same Gln66-Tyr67-Gly68 tripeptide found in WT DsRed. DsRed.T7 matures rapidly with a half-time of ~50 min at 37 °C. Its spectral properties are similar to those of WT DsRed except that a somewhat greater percentage of the chromophores are green (Figure S1). The high solubility of DsRed.T7 suppressed aggregation of the preoxidized intermediate that we used as a starting point for maturation studies. See Table S1 for a full list of the mutations in DsRed.T7.

Slowing Dehydration Increases the Red-to-Green Ratio. In our branched pathway model (Scheme 1C), the branch point intermediate **3** can be dehydrated to enter the green branch of the pathway or can be further oxidized to enter the red branch of the pathway. Therefore, the ratio of red to green chromophores should be determined by the relative reaction rates for **3** to **4g** versus **3** to **4r**, so selectively altering either rate should change the final red-to-green ratio.

To test this prediction, we adapted a procedure that was previously used to study GFP maturation.[17] Incorporating C_β-dideuterated tyrosine into the chromophore slows maturation due to a kinetic isotope effect at the step that generates the $C_\alpha-C_\beta$ double bond. This kinetic isotope effect was shown to involve a dehydration reaction analogous to the **3**-to-**4g** and **5r**-to-**6r** dehydrations in Scheme 1C. Our model predicts that incorporating C_β-dideuterated tyrosine will slow **3** to **4g** but not **3** to **4r**, thereby increasing the final red-to-green ratio (Figure 1A). By contrast, Scheme 1B predicts no change in the red-to-green ratio. For this experiment, a tyrosine auxotrophic *Escherichia coli* strain was transformed to express DsRed.T7, and cells were grown in minimal media supplemented with either normal or C_β-dideuterated tyrosine. To determine the red-to-green ratios, the protein samples were purified and allowed to mature completely at 37 °C. Absorbance spectra were then recorded (Figure 1B). Incorporating C_β-dideuterated tyrosine increased the red-to-green ratio as indicated by a decreased absorbance at 480 nm (Figure 1B). After separating the red and green absorbance spectra (see Experimental Procedures and

(15) Subach, F. V.; Subach, O. M.; Gundurov, I. S.; Morozova, K. S.; Piatkevich, K. D.; Cuervo, A. M.; Verkhusha, V. V. *Nat. Chem. Biol.* **2009**, *5*, 118–126.

(16) Pletnev, S.; Subach, F. V.; Dauter, Z.; Wlodawer, A.; Verkhusha, V. V. *J. Am. Chem. Soc.* **2010**, *132*, 2243–2253.

(17) Pouwels, L. J.; Zhang, L.; Chan, N. H.; Dorrenstein, P. C.; Wachter, R. M. *Biochemistry* **2008**, *47*, 10111–10122.

(18) Rosenow, M. A.; Huffman, H. A.; Phail, M. E.; Wachter, R. M. *Biochemistry* **2004**, *43*, 4464–4472.

(19) Zhang, L.; Patel, H. N.; Lappe, J. W.; Wachter, R. M. *J. Am. Chem. Soc.* **2006**, *128*, 4766–4772.

(20) Strack, R. L.; Strongin, D. E.; Bhattacharyya, D.; Tao, W.; Berman, A.; Broxmeyer, H. E.; Keenan, R. J.; Glick, B. S. *Nat. Methods* **2008**, *5*, 955–957.
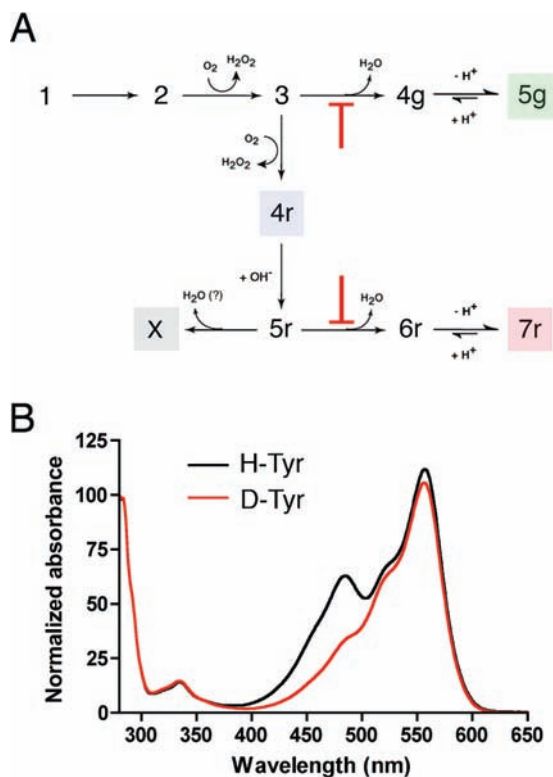
Figure 1. Increase in the red-to-green ratio after slowing dehydration. Normal tyrosine (H-Tyr) or C_β-dideuterated tyrosine (D-Tyr) was incorporated into DsRed.T7, and the protein samples were allowed to mature fully. (A) Simplified version of Scheme 1C. Red bars indicate the dehydration steps that should be slowed by incorporating C_β-dideuterated tyrosine. (B) Absorbance spectra of the two samples normalized to absorbance at 280 nm.

Figure S2), a sample containing C_β-dideuterated tyrosine was found to have 60% fewer green chromophores than an equimolar sample containing normal tyrosine. This result supports the view that a dehydration occurs at the branch point of the maturation pathway.

Unexpectedly, although incorporating C_β-dideuterated tyrosine decreased the amount of green chromophore, it did not increase the amount of red chromophore. A possible explanation is that when the **5r**-to-**6r** dehydration is slowed by incorporating C_β-dideuterated tyrosine, more of the molecules undergo a competing side reaction that converts **5r** to a nonabsorbing species ("X" in Scheme 1C). To explore this possibility, we determined the total chromophore concentration by base denaturation. In 0.1 N NaOH, green and red chromophores are both converted to a species that absorbs at 450 nm with an extinction coefficient of ~44 000 M^{-1} cm^{-1} (refs 9, 21), so chromophore concentration can be measured with reference to total protein concentration. As a control, we confirmed that monomeric enhanced GFP (mEGFP),[22] which is assumed to have 100% chromophore formation, has an extinction coefficient after base denaturation of 43 000 M^{-1} cm^{-1} at 450 nm. The results for DsRed.T7 showed that chromophores were present in 95% of the molecules containing normal tyrosine but in only 61% of the molecules containing C_β-dideuterated tyrosine. Thus, in-

corporating C_β-dideuterated tyrosine dramatically increased the amount of a nonabsorbing species from 5% to 39% of the total DsRed.T7 molecules. We infer that incorporating C_β-dideuterated tyrosine shunts more of the DsRed.T7 molecules to the red branch of the pathway, but many of these molecules subsequently undergo a dead-end side reaction, so the amount of red chromophore does not increase. This interpretation is supported by our quantitative analysis. Specifically, as described below, we find that incorporating C_β-dideuterated tyrosine increased the yield of three products that are predicted to result from the red branch of the pathway: (1) the fraction of molecules that contain either the red chromophore or the nonabsorbing species, (2) the total amount of blue species formed, and (3) the amount of H_2O_2 produced by the final oxidation.

As the first step in this quantitation, we needed to determine the extinction coefficients for the green and red chromophores in the native protein (see Experimental Procedures). These measurements are challenging because the absorbance spectra of the two chromophores overlap. However, Wiedenmann and colleagues described a way to obtain the extinction coefficient for a red chromophore.[23] This method exploits the differential rates of alkaline denaturation for molecules containing green versus red chromophores. At pH 11−13, molecules containing the green chromophore denature faster than molecules containing the red chromophore, so the green chromophore is converted faster than the red chromophore to the 450-nm absorbing species (Figure S3). After all of the green chromophore has been converted, an isosbestic point appears in the spectra, and the subsequent increase in absorbance at 450 nm correlates linearly to the decrease in absorbance of the red chromophore at 558 nm. Because the extinction coefficient for the 450-nm absorbing species is known, the extinction coefficient for the red chromophore can be determined. For DsRed.T7 containing normal tyrosine, we calculated the extinction coefficient for the red chromophore at 558 nm to be 122 500 M^{-1} cm^{-1}, a value similar to previous estimates.[9,23] A nearly identical value was obtained for DsRed.T7 containing C_β-dideuterated tyrosine (Figure S3 and Table 1).

The next step was to obtain the extinction coefficient for the green chromophore in the native protein. On the basis of the total chromophore content and the extinction coefficient for the red chromophore, we estimate that, in mature DsRed.T7 containing normal tyrosine, 52% of the molecules contained a green chromophore, 43% contained a red chromophore, and 5% contained a nonabsorbing species (see Experimental Procedures and Table 1). In turn, based on these values and the spectrally separated absorbance of the green chromophore, we calculated the extinction coefficient for the green chromophore at 480 nm to be 44 000 M^{-1} cm^{-1}, which is similar to the extinction coefficient for GFP.[21,24]

By applying these extinction coefficients to the spectral analysis of mature DsRed.T7 containing C_β-dideuterated tyrosine (Figure S2), we estimate that 20% of the molecules contained a green chromophore and 41% contained a red chromophore, implying that 39% contained a nonabsorbing species (Table 1). This estimate for the nonabsorbing species matches the number obtained by base denaturation (see above), suggesting that our extinction coefficients are reliable.

(21) Ward, W. W. In *Green Fluorescent Protein: Properties, Applications and Protocols*, 2nd ed.; Chalfie, M., Kain, S. R., Eds.; Wiley and Sons: Hoboken, NJ, 2005; pp 39−65.
(22) Zacharias, D. A.; Violin, J. D.; Newton, A. C.; Tsien, R. Y. *Science* **2002**, *296*, 913–916.
(23) Kredel, S.; Nienhaus, K.; Oswald, F.; Wolff, M.; Ivanchenko, S.; Cymer, F.; Jeromin, A.; Michel, F. J.; Spindler, K. D.; Heilker, R.; Nienhaus, G. U.; Wiedenmann, J. *Chem. Biol.* **2008**, *15*, 224–233.
(24) Tsien, R. Y. *Annu. Rev. Biochem.* **1998**, *67*, 509–544.

Table 1. Properties of Fluorescent Proteins Used in This Study[a]

variant	green extinction coefficient (M^{-1} cm^{-1})	red extinction coefficient (M^{-1} cm^{-1})	quantum yield	maturation $t_{1/2}$ at 37 °C (h)	% red	% green	% nonabsorbing
DsRed.T7 (H-Tyr)	44000	122500	0.44	0.83	43	52	5
DsRed.T7 (D-Tyr)	44000	120100	0.44	1.3	41	20	39
DsRed.T7-K83R	41500	--	ND	ND	ND	ND	ND

[a] Listed are values obtained for DsRed.T7 and DsRed.T7-K83R containing normal tyrosine (H-Tyr), and for DsRed.T7 containing C_β-dideuterated tyrosine (D-Tyr). Extinction coefficients for chromophores in the native proteins were determined at the absorbance maxima, which were 480 and 558 nm for the green and red chromophores, respectively (see Figure S2). For comparison, WT DsRed has a quantum yield of 0.7 and a $t_{1/2}$ for maturation of 11 h (ref 25). In mature WT DsRed, the ratio of red to green chromophores is in the range of 1.0−1.5 (refs 9, 13, 32), but the amount of the nonabsorbing species has not been measured. ND, not determined.

Lowering the O_2 Concentration Decreases the Red-to-Green Ratio. O_2 is required for two oxidation steps during red chromophore formation. According to Scheme 1C, the final **3**-to-**4r** oxidation commits the molecule to the red branch of the pathway. This final oxidation is in kinetic competition with the **3**-to-**4g** dehydration, which commits the molecule to the green branch of the pathway. Therefore, lowering the O_2 concentration during maturation should favor the green branch of the pathway, leading to a decrease in the final red-to-green ratio (Figure 2A). Although this experiment cannot distinguish our model from the irreversible deprotonation model (Scheme 1B), it can constrain possible maturation pathways by testing whether the branch point intermediate is the substrate for the final oxidation.

DsRed.T7 was expressed and purified under anaerobic conditions, and was then allowed to mature in buffer equilibrated with 0.02, 0.05, 0.10, 0.20, 0.24, or 21% (atmospheric) O_2. At low O_2 concentrations, overall maturation may be slowed due to kinetic inhibition of the initial **2**-to-**3** oxidation (Figure 2A), so an end point analysis was performed by allowing the samples to mature for 48 h at 37 °C followed by a chase in fully aerated buffer. Absorbance spectra revealed that decreasing the O_2 concentration below 0.20% during maturation progressively decreased the red-to-green ratio (Figure 2B,C), as predicted if the final oxidation occurs at the branch point in the pathway.

To determine whether the loss of red chromophores was matched by a gain of green chromophores, we compared a sample matured in buffer equilibrated with 0.02% O_2 to one matured in fully aerated buffer. Lowering the O_2 concentration led to a 4.15-fold decrease in the amount of red chromophore absorbance and a 1.45-fold increase in the amount of green chromophore absorbance. The ratio of these changes (4.15/1.45 = 2.86) is essentially identical to the ratio of the extinction coefficients for the red and green chromophores (122 500/44 000 = 2.78), indicating the same total number of chromophores was produced under the two maturation conditions. Thus, as predicted by our model, slowing oxidation favors the green branch of the pathway and does not significantly affect production of the nonabsorbing species.

H_2O_2 Is Produced at Early Steps in Chromophore Formation. According to Scheme 1C, oxidation occurs upstream of dehydration in the DsRed maturation pathway. Thus, chromophore formation should lag behind oxidation.[17,19] As an experimental test, we monitored the production of H_2O_2, which is thought to be generated by both of the oxidation steps.[2,9,19] The analysis was performed with DsRed.T7 that had been expressed and purified anaerobically. Oxidation was initiated by transferring purified DsRed.T7 to oxygenated buffer, and maturation was tracked over time by measuring absorbance spectra in parallel with H_2O_2 generation (see Experimental Procedures). Because these kinetic experiments were performed at room temperature, the half-time for red chromophore formation was ~85 min. Figure 3A shows that H_2O_2 production
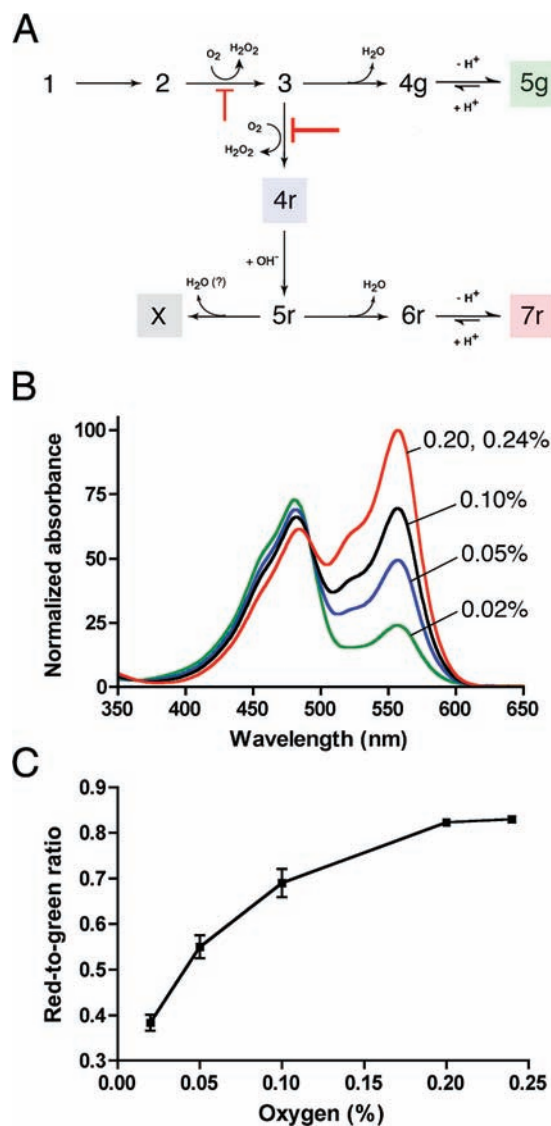

Figure 2. Decrease in the red-to-green ratio after maturation at low O_2 concentrations. (A) Simplified version of Scheme 1C. Red bars indicate the oxidation steps that should be slowed by lowering the O_2 concentration. (B) Absorbance spectra of DsRed.T7 after maturation at the indicated O_2 concentrations. The protein was expressed and purified under anaerobic conditions, then allowed to mature fully in the presence of 0.02−0.24% oxygen. An O_2 concentration of 0.20% corresponded to ~40 O_2 molecules per DsRed.T7 molecule. Spectra were normalized to the peak absorbance at 558 nm of a sample that matured in atmospheric O_2. (C) Ratio of red to green chromophores determined after mathematical separation of the spectra from (B). Error bars indicate SEM for three independent replicates.

reached a plateau by 50 min. At this time point, formation of the green chromophore was incomplete and formation of the
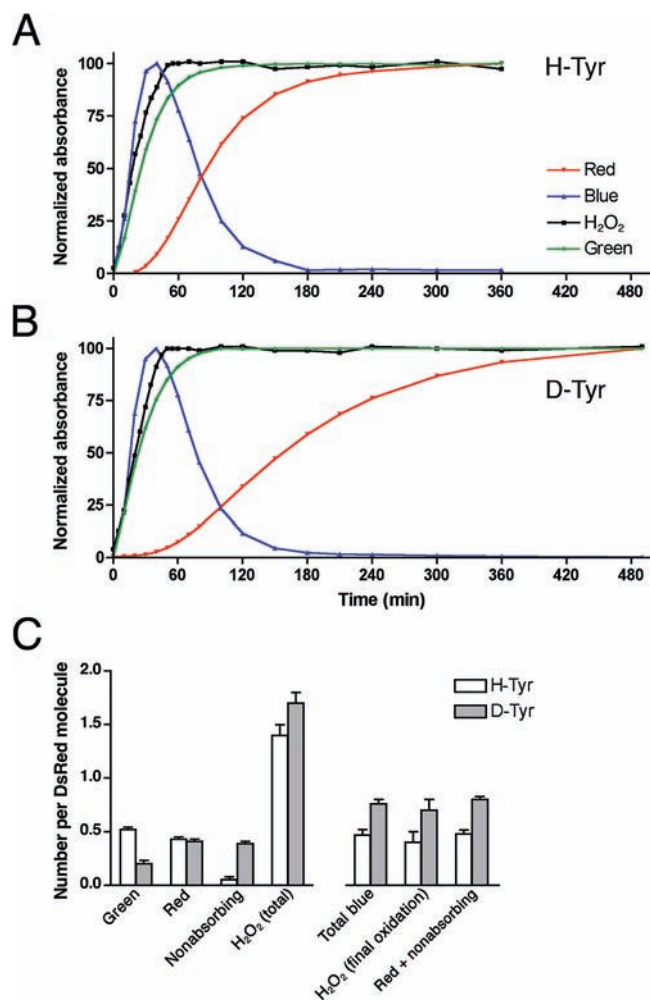
Figure 3. Formation of DsRed species and H_2O_2 after incorporation of normal tyrosine (H-Tyr) or C_β-dideuterated tyrosine (D-Tyr) into DsRed.T7. (A and B) Maturation kinetics at room temperature. Plotted are the peak absorbance signals for the green and red chromophores and the blue species after spectral separation, as well as the amount of H_2O_2 produced as measured by an absorbance assay. Each curve was normalized to the maximal signal obtained. Data from a representative experiment are shown. (C) Absolute amounts of the species formed during maturation of DsRed.T7 in the presence of normal or C_β-dideuterated tyrosine. The amount of H_2O_2 produced during the final oxidation was calculated as the total amount of H_2O_2 produced minus 1.0, because all molecules should have undergone the initial oxidation. The three items on the right are grouped separately because they all demonstrate how incorporating C_β-dideuterated tyrosine shunted molecules to the red branch of the pathway. Error bars indicate SEM for three independent replicates.

red chromophore was just beginning (Figure 3A). This result confirms that oxidation precedes the late steps in chromophore formation.

Quantitation of H_2O_2 levels enabled us to test an additional prediction. We estimate that after incorporating normal tyrosine, 43% of the mature DsRed.T7 molecules contained the red chromophore while 5% contained the nonabsorbing species (Table 1), so according to Scheme 1C, 48% of the molecules underwent the final oxidation along the red branch of the pathway. Thus, maturation should have produced 1.48 molecules of H_2O_2 per molecule of DsRed.T7. Consistent with this prediction, we found that 1.4 ± 0.1 molecules of H_2O_2 were produced per molecule of DsRed.T7 containing normal tyrosine.

Our model makes two further predictions regarding the effects of slowing dehydration by incorporating C_β-dideuterated ty-

rosine. The first prediction is that dehydration occurs downstream of oxidation, so slowing dehydration should slow red chromophore formation but should have little effect on the kinetics of H_2O_2 production (Figure 1A). These results were indeed observed (Figure 3). By contrast, the irreversible deprotonation model postulates that dehydration occurs upstream of the final oxidation (Scheme 1B), in which case slowing dehydration should have delayed the completion of H_2O_2 production. The second prediction of our model is that H_2O_2 production should be enhanced by incorporating C_β-dideuterated tyrosine because more molecules will be shunted to the red branch of the pathway (see above). Specifically, we estimate that, after incorporating C_β-dideuterated tyrosine, 41% of the mature DsRed.T7 molecules contained the red chromophore while 39% contained the nonabsorbing species (Table 1), implying that 80% of the molecules underwent the final oxidation. Thus, maturation should have produced 1.80 molecules of H_2O_2 per molecule of DsRed.T7. Consistent with this prediction, we found that 1.7 ± 0.1 molecules of H_2O_2 were produced per molecule of DsRed.T7 containing C_β-dideuterated tyrosine. The combined results strongly support Scheme 1C.

The Final Oxidation Produces a Blue Species in the Red Branch of the Pathway. As previously observed with WT DsRed,[14] a blue species with an absorption peak at 407 nm forms early and then disappears as the red chromophore forms (Figure 3 and Figure S4). The irreversible deprotonation model proposes that the blue species is the neutral (protonated) form of green chromophore (Scheme 1B), whereas we propose that the blue species is a cyclic imine in conjugation with the acylimine (Scheme 1C). These two models make different predictions about how the kinetics of oxidation will relate to the kinetics of formation and disappearance of the blue species. Scheme 1B predicts that the final oxidation consumes the blue species, so when oxidation is complete, no blue species should remain. By contrast, Scheme 1C predicts that the final oxidation produces the blue species, so the blue species should form throughout the oxidation process and should continue to disappear after oxidation is complete. We found that total formation of the blue species lagged slightly behind oxidation (Figure S5) and that disappearance of the blue species continued long after oxidation was complete (Figure 3), consistent with Scheme 1C.

The two models also differ in their predictions about the effects of slowing dehydration by incorporating C_β-dideuterated tyrosine. Scheme 1B places dehydration upstream of blue species formation, in which case slowing dehydration should slow formation of the blue species but should not affect the total amount of blue species formed. By contrast, Scheme 1C places the **3**-to-**4g** dehydration at the branch point, in which case slowing dehydration should not alter the kinetics of blue species formation but should increase the total amount of blue species formed. The results shown in Figure 3 confirm both predictions of Scheme 1C. First, incorporating C_β-dideuterated tyrosine had virtually no effect on the kinetics of formation of the blue species (Figure 3A,B). Second, incorporating C_β-dideuterated tyrosine increased the total amount of blue species formed by ~1.6-fold (Figure 3C). This value matches the increase in the amount of H_2O_2 produced by the final oxidation, and also matches the increase in the fraction of mature molecules that contained either the red chromophore or the nonabsorbing species (right side of Figure 3C). Therefore, all of our results indicate that slowing dehydration increases the likelihood that the branch point intermediate will be converted to a blue species that is on the red branch of the pathway.

Interestingly, slowing dehydration had no effect on the kinetics of disappearance of the blue species, indicating that dehydration does not directly consume the blue species. As shown in Scheme 1C, we explain this result by proposing that the blue **4r** is rehydroxylated to the colorless **5r**, which is the substrate for dehydration.

Our model makes two further predictions: (1) the blue species should form only on the red branch of the pathway, and (2) the side chain of Tyr67 should not contribute to absorbance of the blue species. We tested these predictions using two point mutants of DsRed.T7. The first mutant was DsRed.T7-K83R, which matures only to the green end point of the pathway.[11] Scheme 1C predicts that no blue species should form in this mutant, whereas Scheme 1B predicts that oxidation should still generate the blue species, which will slowly deprotonate to form the green chromophore. Consistent with Scheme 1C, we detected no blue species during maturation of DsRed.T7-K83R even though green chromophore formation lagged behind oxidation (Figure S6A,B). The second mutant was DsRed.T7-Y67L, which replaces the aromatic Tyr67 side chain with an aliphatic side chain that cannot become part of a chromophore.[18] Thus, fully mature DsRed.T7-Y67L has no visible absorbance. However, Scheme 1C predicts that a transient blue species should form during maturation of DsRed.T7-Y67L, whereas Scheme 1B predicts that no blue species will form. We detected low levels of a transient blue species during maturation of DsRed.T7-Y67L (Figure S6C,D), consistent once again with Scheme 1C.

Kinetic Modeling of DsRed Maturation. We performed global curve fitting of the maturation data by modeling the pathway in Scheme 1C with six rate constants (Figure S7A). A general goal was to determine whether our reaction scheme could account for the experimental results. A more specific goal was to determine whether incorporation of C_β-dideuterated tyrosine selectively altered the rate constants for the postulated **3**-to-**4g** and **5r**-to-**6r** dehydration reactions, corresponding to k_2 and k_6 in Figure S7A.

The inputs to the global curve fitting were the molar quantities of H_2O_2, the green and red chromophores, and the blue and nonabsorbing species. To quantify the amount of the blue species, we needed to know its extinction coefficient. As described in Experimental Procedures and Figure S5, the first step was to determine the total absorbance of the blue species that had formed. We obtained this value by multiplying the rate constant for consumption of the blue species (k_4 in Figure S7A) by the integrated absorbance of the blue species. The next step was to estimate the total moles of blue species that had formed. We obtained this value by assuming that, in DsRed.T7 containing normal tyrosine, the blue species was converted to red chromophore with ~90% efficiency (Table 1). These calculations indicated that the blue species had an extinction coefficient at 407 nm of 43 900 M^{-1} cm^{-1}, which is in the same range as extinction coefficients for the blue intermediates in blue-to-red fluorescent timer variants of DsRed.[15]

The six-step kinetic model provided an excellent fit to the maturation data for DsRed.T7 containing either normal or C_β-dideuterated tyrosine (Figure S7B,C and Table S2). For comparison, the data did not fit a five-step kinetic model in which **4r** and **5r** were treated as a single intermediate in rapid equilibrium. Curve fitting indicated that the slowest steps in red chromophore formation were consumption of the blue species **4r** and dehydration of **5r**, corresponding to k_4 and k_6 in Figure S7A.

Incorporation of C_β-dideuterated tyrosine had a substantial effect only on the two rate constants (k_2 and k_6) that correspond to the dehydration reactions (Table S2). There was a 3.3-fold increase in the half-time for dehydration of **3** to **4g** along the green branch of the pathway, and a 7.7-fold increase in the half-time for dehydration of **5r** to **6r** along the red branch of the pathway. The half-times for the other steps were largely unchanged. These results are consistent with a primary kinetic isotope effect on the dehydration reactions.[17] In sum, the kinetic modeling verifies that Scheme 1C is a plausible pathway for DsRed maturation.

Discussion

The data presented here strongly support the existence of a novel branched pathway that generates the green and red chromophores in DsRed (Scheme 1C). This work builds upon prior studies of chromophore maturation in DsRed and GFP.[9,11,14,17,19] The key concept in our model is that the branch point intermediate can undergo two competing reactions: dehydration to enter the green branch of the pathway, or a final oxidation to enter the red branch of the pathway. This final oxidation is proposed to generate the blue species originally observed by Verkhusha and colleagues.[14] Here, we have confirmed four major predictions of the new model.

The first prediction is that slowing dehydration should favor the final oxidation, thereby shunting more molecules to the red branch of the pathway. In support of this idea, formation of the green chromophore was dramatically reduced by incorporating C_β-dideuterated tyrosine, which selectively slowed dehydration due to a kinetic isotope effect.[17] Moreover, slowing dehydration enhanced the production of H_2O_2, presumably because more molecules underwent the final oxidation.

The second prediction is that lowering the O_2 concentration should favor dehydration of the branch point intermediate, thereby shunting more molecules to the green branch of the pathway. Indeed, lowering the O_2 concentration enhanced green chromophore formation at the expense of red chromophore formation.

The third prediction is that both of the oxidation reactions should occur upstream of dehydration. In support of this idea, slowing dehydration had no effect on the kinetics of oxidation as measured by H_2O_2 production. Moreover, H_2O_2 production was faster than chromophore formation, indicating that oxidation occurs upstream of the late steps in the maturation pathway.

The fourth prediction is that the blue species is produced by the final oxidation step and is on the red branch of the pathway. We found that formation of the blue species lagged slightly behind H_2O_2 production, and that disappearance of the blue species continued after oxidation was complete. These results support the idea that oxidation produces the blue species but does not consume it. Moreover, no blue species was detected during maturation of a green-only point mutant, as expected if the blue species is a precursor of the red chromophore but not of the green chromophore.

These qualitative observations were extended by showing that our data quantitatively fit Scheme 1C. We calculated the amounts of the red and green chromophores, the blue species, and H_2O_2 during the time course of maturation for DsRed.T7 containing normal or C_β-dideuterated tyrosine, and then performed global curve fitting. The theoretical curves fit the experimental data very well.

Our analysis indicates that the slowest steps in the red branch of the pathway occur after acylimine formation. If Scheme 1C is accurate, these slow steps are hydroxylation of the blue species **4r**

to **5r** and subsequent loss of the hydroxyl group during dehydration of **5r** to **6r**. Interestingly, hydroxylation of **4r** to **5r** is analogous to hydroxylation of the cyclic imine in the equilibrium mixture that comprises intermediate **3**, yet our data suggest that hydroxylation is rapid and reversible prior to acylimine formation but much slower after acylimine formation. We speculate that, because acylimine formation extends the conjugated system that is disrupted by hydroxylation, the energy barrier for hydroxylation is higher after acylimine formation. Reactions at the transiently hydroxylated heterocycle carbon are thought to be facilitated by Glu215, which is analogous to Glu222 in GFP.[6] In rapidly maturing DsRed variants,[25] the N42Q mutation repositions Glu215 relative to the heterocycle[26] (Figure S8), and this change may enhance the rate-limiting hydroxylation and dehydration steps in red chromophore formation.

During maturation of wild-type DsRed and some of the blue-to-red fluorescent timers, the blue species persists for hours,[14,15] suggesting that for certain variants the **4r**-to-**5r** reaction that consumes the blue species is the slowest step in the pathway. In such a situation, illumination of the blue species with violet light may accelerate maturation. Such a light-driven acceleration has been observed for tetrameric DsRed variants,[14] and might play in a role in the activation of photoactivatable mCherry.[27]

Our model differs from the irreversible deprotonation model in crucial ways. Notably, our model postulates that the transient blue species is a cyclic imine in conjugation with the acylimine (Scheme 1C), whereas the irreversible deprotonation model postulates that the blue species is the neutral (protonated) form of the green chromophore (Scheme 1B). The following results contradict predictions of the irreversible deprotonation model. (1) Slowing dehydration increased the red-to-green ratio. (2) Slowing dehydration did not delay the completion of oxidation. (3) Slowing dehydration did not slow formation of the blue species but did increase the total amount of blue species formed. (4) After oxidation was complete, a substantial amount of the blue species remained and then gradually disappeared. (5) No blue species was detected during maturation of the green-only DsRed.T7-K83R mutant. (6) A blue species was detected during maturation of the DsRed.T7-Y67L mutant, which cannot generate the green chromophore. The combined data convincingly rule out the irreversible deprotonation model.

Similar reasoning allows us to evaluate a more recent maturation scheme based on studies of blue-to-red fluorescent timer variants of DsRed.[15] The blue species was postulated to be the acylimine in conjugation not with a cyclic imine, as we have proposed, but rather with an aromatic α-enolate.[16,28] A crucial distinction between these two possibilities is that, with an aromatic α-enolate, the final oxidation would consume the blue species while generating the $C_\alpha-C_\beta$ double bond that incorporates the phenolic group into the conjugated structure.[16] The following results from our work are inconsistent with this idea. (1) After oxidation was complete, a substantial amount of the blue species remained and then gradually disappeared, implying that the final oxidation occurs upstream rather than downstream of the blue species. (2) Incorporating C_β-dideuterated tyrosine did not alter the kinetics of oxidation, implying

that O_2 is not consumed during the step that generates the $C_\alpha-C_\beta$ double bond.[17] Thus, we suggest that the older cyclization-dehydration-oxidation model is no longer valid, and that the data fit much better to a cyclization-oxidation-dehydration model.

One issue that remains mysterious is the identity of the nonabsorbing species that forms as a dead-end product from the red branch of the pathway ("X" in Scheme 1C). This species previously escaped notice because under normal conditions, only a small fraction of the mature DsRed molecules are nonabsorbing. Incorporating C_β-dideuterated tyrosine dramatically increased production of the nonabsorbing species. We infer that the nonabsorbing species is produced by a side reaction that competes with dehydration. The nature of this side reaction is unknown. In some DsRed variants the immature chromophore can undergo hydrolysis reactions,[16] and this process may be enhanced by incorporating C_β-dideuterated tyrosine. Another possibility is that the nonabsorbing species arises from an alternative dehydration that does not involve C_β of Tyr67.

This study provides a general framework for understanding fluorescent protein maturation. Our work was inspired by the scheme for GFP maturation from Wachter and colleagues, who argue persuasively that the phenolic group is incorporated into the chromophore not by an oxidation step, but rather by a dehydration step.[6,17−19] All of our data are consistent with this view of chromophore formation. We have extended the cyclization-oxidation-dehydration concept to explain the existence of both green and red chromophores in mature DsRed. By analogy, the results and approaches described here will be useful for dissecting the remarkable variety of chemical reactions that take place in other fluorescent proteins.[1−4]

Experimental Procedures

Expression Plasmids. Regulatable bacterial expression was obtained using pQE-81 (Qiagen), which contains the *lacI^q* gene and encodes an N-terminal hexahistidine tag. The DsRed.T7 gene was inserted into this plasmid to create pQE-81-DsRed.T7. Site-directed mutagenesis introduced substitutions to create pQE-81-DsRed.T7-K83R and pQE-81-DsRed.T7-Y67L. All constructs were confirmed by sequencing. A folder of annotated GenBank-style sequence files for these plasmids is included in the Supporting Information.

Anaerobic Expression and Purification of DsRed.T7 and Its Derivatives. To express DsRed.T7 or one of its derivatives under anaerobic conditions, the tyrosine auxotrophic *E. coli* strain WU38 (Yale CGSC no. 5975) was transformed with the appropriate expression plasmid, and a 250-mL culture was grown in M9 minimal media supplemented with 100 mg/L normal L-tyrosine (Sigma) or C_β-dideuterated-L-tyrosine (Cambridge Isotope Laboratories) and 200 μg/mL ampicillin in a baffled flask. When the culture reached an OD_{600} of ~1.0, it was vacuum degassed for 20 min to remove most of the O_2. The culture was then poured into sealed tubes, and the cells were allowed to consume the residual O_2 by incubating them with shaking at 37 °C for 30 min. Expression was then induced by injecting IPTG into the sealed tubes to a final concentration of 1 mM and incubating with shaking at 37 °C for 8−12 h.

To purify DsRed.T7 or one of its derivatives under anaerobic conditions, the induced culture in its sealed tubes was transferred to an ice water bath for 30 min. All subsequent manipulations took place at 4 °C. Cells were centrifuged at 3000*g*, and the cell pellets were lysed in a solution of BPER II (Pierce) and 0.5 M NaCl that had been deoxygenated by adding 56 mM glucose, 100 nM glucose oxidase, and 1.5 μM catalase.[29] The total volume of lysis solution was 14 mL. Lysis was performed for 20 min with gentle shaking.

(25) Bevis, B. J.; Glick, B. S. *Nat. Biotechnol.* **2002**, *20*, 83–87.
(26) Strongin, D. E.; Bevis, B.; Khuong, N.; Downing, M. E.; Strack, R. L.; Sundaram, K.; Glick, B. S.; Keenan, R. J. *Protein Eng. Des. Sel.* **2007**, *20*, 525–534.
(27) Subach, F. V.; Malashkevich, V. N.; Zencheck, W. D.; Xiao, H.; Filonov, G. S.; Almo, S. C.; Verkhusha, V. V. *Proc. Natl. Acad. Sci. U.S.A.* **2009**, *106*, 21097–21102.
(28) Piatkevich, K. D.; Verkhusha, V. V. *Curr. Opin. Chem. Biol.* **2010**, *14*, 23–29.

(29) Aitken, C. E.; Marshall, R. A.; Puglisi, J. D. *Biophys. J.* **2008**, *94*, 1826–1835.

The lysate was then centrifuged at 10 000g, and the supernatant was added to Ni-NTA agarose beads (Qiagen) in a 15-mL conical tube. The hexahistidine-tagged protein was mixed with the Ni-NTA agarose beads for 5 min to allow binding. After centrifugation at 2000g for 1 min, the beads were washed once with 14.5 mL of vacuum degassed wash buffer #1 (20 mM imidazole, pH 7.5, 1 M NaCl, 0.5% Triton X-100, and 0.1% NaN$_3$) and once with vacuum degassed wash buffer #2 (20 mM imidazole, pH 7.5, 300 mM NaCl, and 0.1% NaN$_3$). Protein stored under these conditions remained colorless even if incubated for 36 h at 37 °C, indicating that the oxygen depletion was efficient.

Maturation assays were performed after eluting the purified protein from the Ni-NTA agarose beads. For elution, the beads were mixed for 5 min in degassed buffer containing 250 mM imidazole, pH 7.5, 300 mM NaCl, and 0.1% NaN$_3$. Then the Ni-NTA agarose was removed by centrifugation, and the eluted protein solution was added directly to a 10-mL spin-desalt column (Pierce) equilibrated with oxygenated room temperature maturation buffer (5 mM Na$^+$-HEPES, pH 7.4, and 100 mM NaCl). A typical elution yielded 2 mL of solution with a protein concentration of ~10 μM as determined using the BCA assay (Pierce). For DsRed.T7 and DsRed.T7-Y67L, the maturation assays were initiated at this point. For DsRed.T7-K83R, an additional centrifugation was first performed at 4 °C for 5 min at 12 000g to remove aggregates.

Maturation of DsRed.T7 under Low O$_2$ Conditions. DsRed.T7 was expressed and bound to Ni-NTA agarose beads under anoxic conditions as described above, but the protein was not eluted from the beads. Instead, immature DsRed.T7 bound to Ni-NTA agarose beads was aliquoted into glass vials (~15 mL volume) with airtight lids. The vials were vacuum degassed and then flushed with mixtures of air and N$_2$ to give final O$_2$ concentrations (v/v) of 0.02−0.24%. A fully aerated (~21% O$_2$) control sample was also prepared. The vials were incubated for 48 h at 37 °C to allow maturation. Then, the mature protein samples were eluted, buffer exchanged using Amicon Ultra centrifugal filters (Millipore) into aerated maturation buffer, and chased at 37 °C for 6 h to ensure complete maturation.

Measurement and Analysis of Absorbance Spectra. Absorbance spectra were measured using a Lambda 25 UV/vis spectrophotometer (Perkin-Elmer). For tracking maturation, the spin-desalted protein solution (see above) was transferred immediately to a cuvette in the spectrophotometer, and spectra were collected at appropriate intervals. All of the time-course experiments were performed at room temperature.

To determine the contributions of the red and green chromophores and the blue species to the composite absorbance spectra, the SIMPLISMA algorithm[30] was used within the UV-IR Manager software (ACD). The absorbance spectra from a maturation time course for DsRed.T7 containing normal tyrosine were imported into the software. Absorbance values between 360 and 650 nm were used for spectral separation using component content analysis. As a control, the calculated absorbance spectrum of the green chromophore was overlaid with the absorbance spectrum of the green-only DsRed.T7-K83R mutant and found to be nearly identical (see Figure S2).

Determination of Extinction Coefficients. To determine the extinction coefficient for the red chromophore in DsRed.T7, we used a time-dependent alkaline denaturation method[23] as described in Results and Figure S3. Briefly, concentrated samples of mature DsRed.T7 (~10 mg/mL) in 5 mM Na$^+$-HEPES, pH 7.4, and 100 mM NaCl were diluted 1:100 into 100 mM NaCl adjusted to pH 12 with NaOH. Absorbance spectra were then recorded every 5 min for

4 h, followed by a final measurement at 24 h. Spectra collected between 1.0 and 2.5 h (after appearance of the isosbestic point) were used for the analysis. For each time point relative to the previous time point, we computed the ratio of increase in absorbance at 450 nm to decrease in absorbance at 558 nm. The average value of these ratios was then used, together with the known extinction coefficient for the 450 nm-absorbing species, to determine the extinction coefficient for the red chromophore at 558 nm (Table 1).

To determine the extinction coefficient for the green chromophore in DsRed.T7, we needed to know the percentage of molecules that contained the green chromophore. This number was inferred by determining the percentage of molecules that contained either the red chromophore or the nonabsorbing species, and then assuming that the remaining molecules contained the green chromophore. To determine the percentage of molecules that contained the red chromophore, we divided the molar absorbance of the DsRed.T7 sample at 558 nm by the calculated extinction coefficient for the red chromophore. To determine the percentage of molecules that contained the nonabsorbing species, we used base denaturation as described in Results to compare total chromophore concentration to total protein concentration. As an example, with DsRed.T7 containing normal tyrosine, we estimated that 43% of the molecules contained the red chromophore and 5% contained the nonabsorbing species, so 52% of the molecules contained the green chromophore. The next step was to calculate the absorbance at 480 nm due to the green chromophores in the DsRed.T7 sample. This value was obtained by spectral separation as shown in Figure S2. By combining the absorbance due to the green chromophore with the percentage of molecules containing the green chromophore, we could estimate the extinction coefficient for the green chromophore at 480 nm.

To determine the extinction coefficient for the transient blue species, the spectrally separated peak absorbance values of the blue species were integrated numerically using Prism software from 0 to 180 min during maturation of DsRed.T7 containing normal tyrosine. This integrated value was multiplied by the rate constant k_4 for blue species consumption, yielding the absorbance of the total amount of blue species that had formed (see Figure S5). From Table 1, we assume that ~90% of the blue species eventually yielded red chromophore with the remainder yielding the nonabsorbing species. The amount of red chromophore in the mature protein was determined using the measured end point value of absorbance at 558 nm plus the extinction coefficient for the red chromophore. At this point, we had estimates for the total moles of blue species that had formed and the corresponding absorbance, so we could estimate the extinction coefficient for the blue species.

Quantitation of H$_2$O$_2$ Production. The PeroXOquant kit (Pierce) was used to measure H$_2$O$_2$ production. This assay takes place at low pH in 25 mM H$_2$SO$_4$, and the final product is a complex between Fe^{3+} and xylenol orange that absorbs at 595 nm. The low pH of the working solution denatures the protein, arresting maturation and abolishing any absorbance from the chromophores at 595 nm.

To monitor H$_2$O$_2$ production, DsRed.T7 or DsRed.T7-K83R was expressed and purified under anoxic conditions as described above, and then divided into two aliquots. One aliquot was placed in the spectrophotometer to follow maturation. At each time point, a small volume from the second aliquot was removed and mixed with the PeroXOquant working solution to measure the accumulated H$_2$O$_2$. This assay required a 20-min incubation, but no new H$_2$O$_2$ was generated during this time because the protein was denatured. Absorbance at 595 nm was measured in 96-well plates for three replicates per time point using a Tecan Safire^2 plate reader. To determine background absorbance values, an identical aliquot was taken at each time point and added to a reaction mixture lacking xylenol orange. These background values were then subtracted from the measurements. As a control to confirm that H$_2$O$_2$ was stable in the maturation buffer, a fresh 5 μM H$_2$O$_2$ stock solution in maturation buffer was assayed at the beginning of the experiment

(30) Bogomolov, A.; Hachey, M.; Williams, A. In *Progress in Chemometrics Research*; Pomerantsev, A. L., Ed.; Nova Science Publishers: Hauppauge, NY, 2005; pp 119−135.

(31) Barondeau, D. P.; Tainer, J. A.; Getzoff, E. D. *J. Am. Chem. Soc.* **2006**, *128*, 3166–3168.

(32) Yarbrough, D.; Wachter, R. M.; Kallio, K.; Matz, M. V.; Remington, S. J. *Proc. Natl. Acad. Sci. U.S.A.* **2001**, *98*, 462–467.

and then after every hour. No change was observed during the 6−8 h time course of the experiment.

For quantitation, standards were prepared from a 30% stock H_2O_2 solution (ACROS) that lacked stabilizers and was stored in the dark at 4 °C. This stock solution was verified using an extinction coefficient at 240 nm of 43.6 M^{-1} cm^{-1}, according to the instructions in the PeroXOquant kit protocol. A standard curve was generated in the linear range of the assay with 0, 2.5, 5.0, 10, 20, 30, 40, and 50 μM H_2O_2. The amount of H_2O_2 produced during each maturation experiment was then determined using this curve. After full maturation of a fluorescent protein sample, the end point value for H_2O_2 concentration was compared to the protein concentration as determined by the BCA assay, yielding the molecules of H_2O_2 produced per molecule of protein. As a control, the green-only DsRed.T7-K83R mutant produced 0.9 ± 0.1 molecules of H_2O_2 per molecule of protein, consistent with the theoretical value of 1.0 that is expected because a single oxidation step occurs during green chromophore formation.

Kinetic Modeling and Global Curve Fitting. Berkeley Madonna software version 8.2 (http://www.berkeleymadonna.com) was used to model a six-step mechanism for DsRed maturation (Figure S7A). The concentrations of seven protein species plus H_2O_2 were modeled with six rate constants using the following equations:

$$d[\mathbf{2}]/dt = -k_1[\mathbf{2}]$$

$$d[\mathbf{3}]/dt = k_1[\mathbf{2}] - k_2[\mathbf{3}] - k_3[\mathbf{3}]$$

$$d[\mathbf{5g}]/dt = k_2[\mathbf{3}]$$

$$d[\mathbf{4r}]/dt = k_3[\mathbf{3}] - k_4[\mathbf{4r}]$$

$$d[\mathbf{5r}]/dt = k_4[\mathbf{4r}] - k_5[\mathbf{5r}] - k_6[\mathbf{5r}]$$

$$d[\mathbf{X}]/dt = k_5[\mathbf{5r}]$$

$$d[\mathbf{7r}]/dt = k_6[\mathbf{5r}]$$

$$d[H_2O_2]/dt = k_1[\mathbf{2}] + k_3[\mathbf{3}]$$

The deprotonation reactions were assumed to be rapid, with essentially all of the mature chromophores deprotonated at equilibrium.

For each time point, data for the blue species and for the green and red chromophores were obtained using spectral separation, and were adjusted based on extinction coefficients to units of molecules per DsRed.T7 molecule. Similarly, the H_2O_2 production data were normalized to the end point amount of H_2O_2 produced per DsRed.T7 molecule. The end point value for the nonabsorbing species ("X") was also included.

Initial guesses for all rate constants before curve fitting were 0.05 min^{-1}. The global curve fitting results were essentially identical regardless of the values of these initial guesses or the choice of curve fitting algorithm. k_4 was allowed to vary, but the results were not significantly changed if k_4 was fixed at the value obtained previously for exponential decay of the blue species (see Figure S5). Each data set was treated independently, and average and standard deviation values were obtained from curve fitting of three independent data sets each for DsRed.T7 containing normal tyrosine or C_β-dideuterated tyrosine (Table S2).

Supporting Information Available: Additional information as noted in text (PDF and zip files). This material is available free of charge via the Internet at http://pubs.acs.org.

JA1030084